

Study of $\text{CO}_2^+(\text{CO}_2)_n$ Cluster in a Paul Ion Trap

L. Karimi¹, S. M. Sadat Kiai^{2,*}, A. R. babazaheh¹, M. Elahi², and S. R. Shafaei²

¹Department of Chemistry, University of Zanjan, Zanjan 45371-38791, Iran

²Nuclear Science and Technology Research Institute (NSTR), Plasma and Nuclear Fusion Research School, A.E.O.I., Tehran 14155-1339, Iran

Received September 28, 2018; Revised November 10, 2018; Accepted November 25, 2018

First published on the web March 31, 2019; DOI: 10.5478/MSL.2019.10.1.27

Abstract : In this article, the properties of $\text{CO}_2^+(\text{CO}_2)_n$ clusters in a Paul ion trap have been investigated using mass-selective instability mode which conducted by chosen precursor ions, mainly Ar^+ and CO_2^+ produced by a mixture of Ar and CO_2 . Exposure of CO_2^+ ions to CO_2 molecules, lead to the formation of $\text{CO}_2^+(\text{CO}_2)_n$ clusters. Here, Ar gas react as a buffer gas and lead to form $\text{CO}_2^+(\text{CO}_2)_n$ cluster by collisional effect.

Keywords : Paul ion trap, ion clusters, time of flight, buffer gas, collisional effect

Introduction

Properties of clusters are valuable in many fields of physics, chemistry (e.g. catalysis) and nanotechnology. Their properties depend on the charge, size, and species (atomic, polyatomic and molecular). Rate of cluster's formation is high, and their timescale is limited to a few microseconds. However, some processes such as cooling and chemical reactions cause to reduce of formation's rate so cluster formation may occur in a longer timescale (millisecond to second).¹⁻³

Cluster ions are defined as a combination of a core ion bound in which a van der Waals force governs to one or more neutral atoms and molecules.⁴ Carbon dioxide is a major gas phase pollutant "greenhouse effect" on the atmosphere; therefore, investigating of monomeric and clustered CO_2 structure study is of particular importance.⁵ In addition, the effect of Ar and Ne gases cause the formation of $\text{CO}_2^+(\text{CO}_2)_n$ clusters and have been studied in reference.⁶

Based on a previous study,⁷ formation of $\text{CO}_2^+(\text{CO}_2)_n$ clusters have a particularly large rate constant. Clusters have very different properties from the isolated atoms/

molecules or bulk materials and can constitute a new type of material. In order to produce clusters, one can either aggregate smaller systems (atoms, molecules, small clusters) or break larger systems.⁷⁻⁹ According to reference 10, the small ion clusters that have a fewer number of atoms (n), could be formed during the first 200 ns and take longer time to disappear them.

Small water cluster ions $\text{H}^+(\text{H}_2\text{O})_{3,4}$ using a three-dimensional quadrupole ion trap (Paul ion trap), has been demonstrated by Lovejoy and Bianco. They were shown this cluster formed in around of 300-500 K.¹¹ They use an ion trap because the ion trap offers the possibility of storing ions in a limited time and a well-defined space range.¹² However, other devices, for instance, Penning traps,^{13,14} quadrupole or multipole linear traps,¹⁵ ion storage rings (electrostatic or magnetic¹⁶ and electrostatic ion beam traps) are also employed.^{17,18} Formation of cluster molecular ions in a Paul ion trap is practical when the confined ions interact in the applied rf fields. The space charges and binary collisions yield to restrict the number of confinement of cluster ions in an ion trap.

In this article, we examine the capability of our Paul ion trap to produce $\text{CO}_2^+(\text{CO}_2)_n$ cluster ions. Some parameters such as volume percentage of CO_2 mixed with Ar gases and radiofrequency voltages have been analyzed. Here, the noble gas Ar plays as a buffer gas that it causes cooling with inelastic collisions.^{19,20}

Experimental

Paul ion trap analyzer

The homemade Paul ion trap electrodes are made of stainless steel 316 with $z_0 = 0.707$ cm, that it is one-half the shortest separation of the endcap electrodes and $r_0 = 1$ cm, is

Open Access

*Reprint requests to S. M. Sadat Kiai
E-mail: sadatkiai@yahoo.com

All MS Letters content is Open Access, meaning it is accessible online to everyone, without fee and authors' permission. All MS Letters content is published and distributed under the terms of the Creative Commons Attribution License (<http://creativecommons.org/licenses/by/3.0/>). Under this license, authors reserve the copyright for their content; however, they permit anyone to unrestrictedly use, distribute, and reproduce the content in any medium as far as the original authors and source are cited. For any reuse, redistribution, or reproduction of a work, users must clarify the license terms under which the work was produced.

the ring electrode radius. The ring electrode has three meshes that involve nine holes with the 0.1 mm diameter and they are around a circle. These meshes are used to entrance of gas to the trap. They are placed 120 degrees apart from each other.²

A cylinder with a volume of $4.64 \times 10^{-3} \text{ m}^3$ was used for the source gas with capacity of 5 bar. Once the cylinder is filled with a mixture of Ar and CO₂ gases, the cylinder output is fed to the small stainless steel tubes, 0.5 mm in diameter. There are three tubes to import the mixed gases to the ionization volume inside the trap. This technique effectively provides a better ionization efficiency and consumes less gases.

There are six small holes, which are 0.1 mm diameter in the center of the lower end-cap electrode, to let the electrons cross into the trap ionization volume. Also, the upper end-cap electrode has the same holes for the passage of ions to the detector. The ion trap has hyperbolic geometry that it was estimated to have higher confinement efficiency. The motion of the ion in a Paul ion trap is described by the Mathieu equations and in r and z directions are given as:

$$\frac{d^2 r}{d\xi^2} + (a_r - 2q_r \cos 2\xi)r = 0 \quad (1)$$

$$\frac{d^2 z}{d\xi^2} + (a_z - 2q_z \cos 2\xi)z = 0 \quad (2)$$

$$a_z = -2a_r = \frac{4qU}{MZ_0^2\Omega^2} \quad (3)$$

$$q_z = -2q_r = \frac{-2qV}{MZ_0^2\Omega^2} \quad (4)$$

$$\xi = \frac{\Omega t}{2} \quad (5)$$

where U is the direct voltage, V is the alternating radiofrequency voltage, q is the electric charge, M is the mass of ion, Z_0 is the one-half the shortest separation of the endcap electrodes and Ω ($\Omega = 2\pi f$) is the angular frequency.²¹ Ions are produced in the trap by an impact of electron ionization technique. In general, the process of ion trap operation consists of pulse ionization, rf voltage scanning and data collection to produce peaks.^{22,23}

Experimental setup and measurements

The experimental set up is depicted in Figure 1. The Paul ion trap is placed in a vacuum chamber with a volume of 0.0147 m^3 and pumped through a turbo-pack up to a

pressure of 10^{-5} mbar. The rf voltage is connected between the ring and end-cap electrodes and operated in the mass-selective instability mode; only radio frequency voltage is applied to the ring electrode. The electrons can be provided through an electron gun, which is situated below the lower end-cap electrode. The Tungsten filament can use 0.46 A, with 9 V and a constant current circuit generates a constant flow of electrons. Also, electron acceleration is made through -110 V. We have applied the ejection voltage, up to -300 V, between Faraday-cup detector and the grid earth. The rf voltage produces more than $-600 V_{0 \rightarrow p}$ (zero to pick) voltage with the frequency up to 1.1 MHz. The entire experiments can be adjusted through 10 canal circuit with LVTTTL and controlled through Labview program.

The output signals obtained from detector were visualized and memorized in oscilloscope. They can provide 200 data on the excel software and can be used as a data for Origin-pro software. Table 1 shows various ionization energies of some gases which employed in the present work.

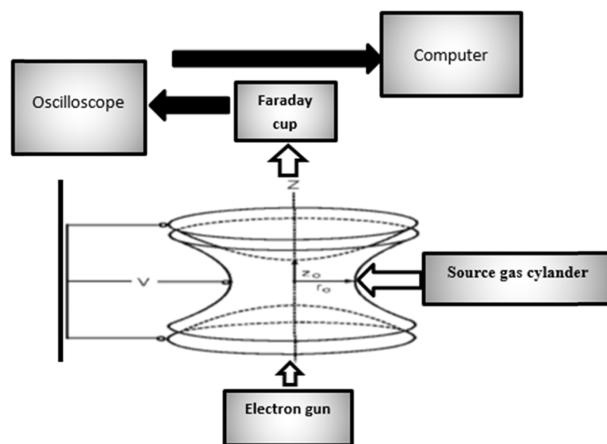


Figure 1. Schematic of experimental set up.

Table 1. Ionization energies (in eV) of different gases²⁰

	Ar	H ₂ O	O ₂	CO ₂
Ionization energies (eV)	15.76	12.62	12.1	13.8

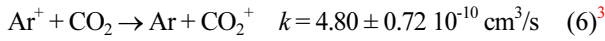
The characteristics of our working gases, Ar and CO₂, also, are shown in Table 2. Carbon dioxide CO₂ was with high purity ($\geq 99.999\%$), and the oxygen and moisture content was low in a chamber ($\approx < 2$ ppm).

Table 2. Physical properties of CO₂ and Ar capsule

Gas	CO ₂	O ₂ +Ar	N ₂	THC	H ₂	H ₂ O
CO ₂	$\geq 99.999\%$	≤ 1 ppm	≤ 3 ppm	≤ 4 ppm	≤ 0.5 ppm	≤ 1 ppm
Gas	Ar	H ₂ O	N ₂	CO ₂ + CO	O ₂	
Ar	99.999%	≤ 2 ppm	≤ 5 ppm	≤ 0.5 ppm	≤ 2 ppm	

Results and discussion

Here, Ar was employed as a buffer gas and ultimately, Ar^+ ions can transfer their charge to CO_2 molecules in less than 1 ns. So, it is the best option for this work:



Effect of various parameters

- Gases ratio $\left(\frac{\text{Ar}}{\text{CO}_2}\right)$

Figure 2, shows a typical Ar signal. It was obtained directly from the oscilloscope. The ejection voltage can be applied either when the rf voltage is completely stopped or during its working regime. Regarding to a fixed rf frequency, several parameters can have influence on the output signal such as gas pressure, ionization time, rf

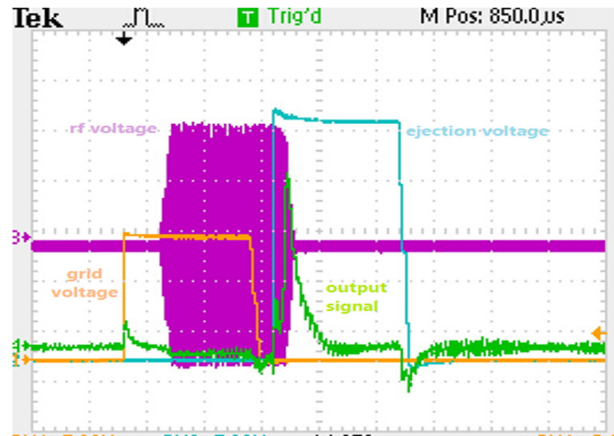


Figure 2. A typical Ar ions output signal (Purple: Radio frequency, Blue: Extraction voltage, Orange: Grid voltage, Green: Ion signal)

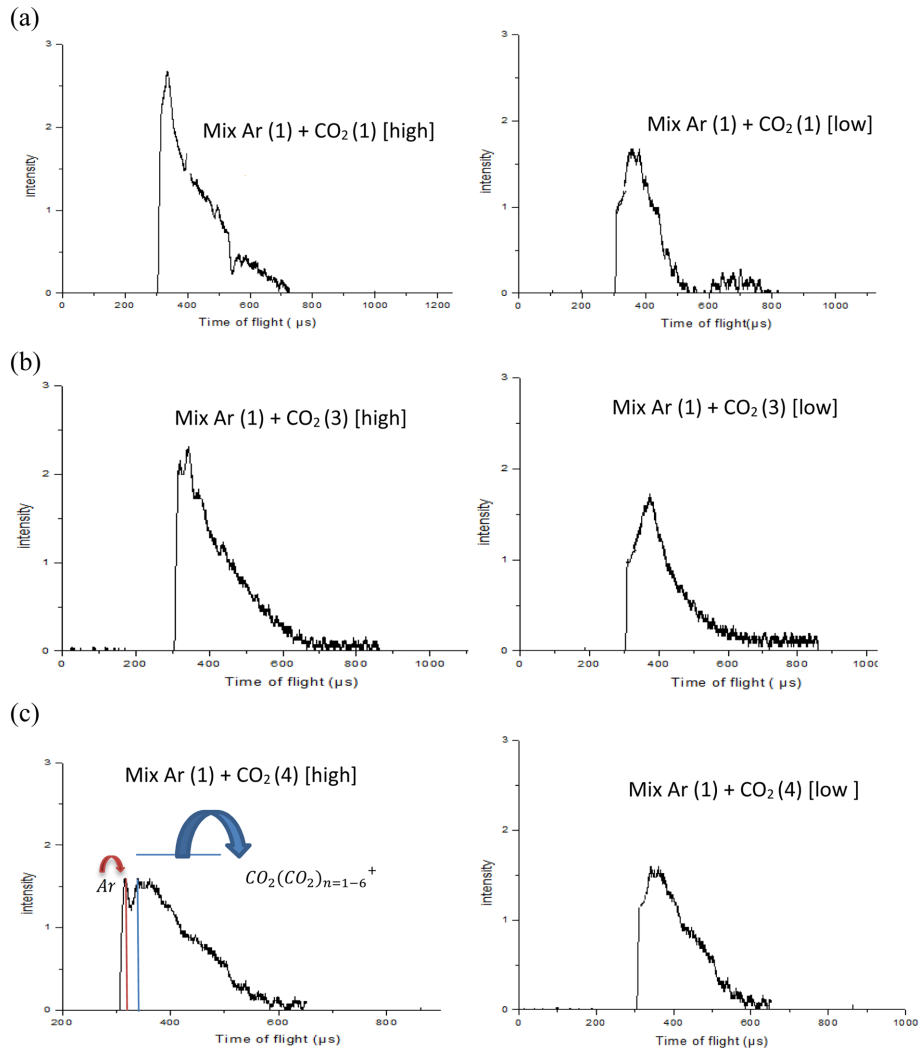


Figure 3. Signals from gas mixture of Ar and CO_2 for low and high rf voltages. (a) Mix Ar (1) + CO_2 (1) in high (left) and low (right) voltage, (b) Mix Ar (1) + CO_2 (3) in high (left) and low (right) voltage, (c) Mix Ar (1) + CO_2 (4) in high (left) and low (right) voltage

voltage, and the ejection position and voltages. Nevertheless, some of best condition have been chosen for the experiment.

Numerous experimental papers have been published visualizing the formation of $\text{CO}_2^+(\text{CO}_2)_n$ ion clusters with the following gas ratios; $\text{Ar}:\text{CO}_2 = 1:4, 1:3, \text{ and } 1:1$. But for this work, we have used low and high rf voltages for the experiments. Figure 3 shows peaks with low rf voltage, no ion clusters are present. However, at the higher rf voltage, the ion cluster signals are present and, no ion clusters appeared after 600-700 μs of the ejection voltage.

According to Figure 3, and the time of flight formula, $m_2 = m_1 \times (t_2/t_1)^2$, the first peak is identified as Ar^+ , then, the other peaks are related to $\text{CO}_2^+(\text{CO}_2)_n$ with $n = 1 - 6$. As seen, for the equal gas mixture proportions, the cluster peak is not clear (see Figure 3(a)), this is also true for the

conditions of $\text{Ar} + 1 \text{ bar } \text{CO}_2$. Formation of small flat top appeared at the higher rf voltages and depicted in Figure 3(a)-(c). Accordingly, they are decreasing as the rf voltage is stopped. During the ejection time, the heavier of cluster ions are expected. Indeed, this is due to the beam character of the ion's cloud during the run down toward the detector through travelling distance of $\sim 4 \text{ cm}$ to the detector through the upper end cup holes.

One of the important reaction of CO_2^+ with the gas molecules is a three body reaction, leading to the formation of a $\text{CO}_2^+(\text{CO}_2)_n$, $n = 2,^{24}$



The influence of damping force on the ion motion has been studied with q_z values ($q_z = 0.45$) near the adiabatic

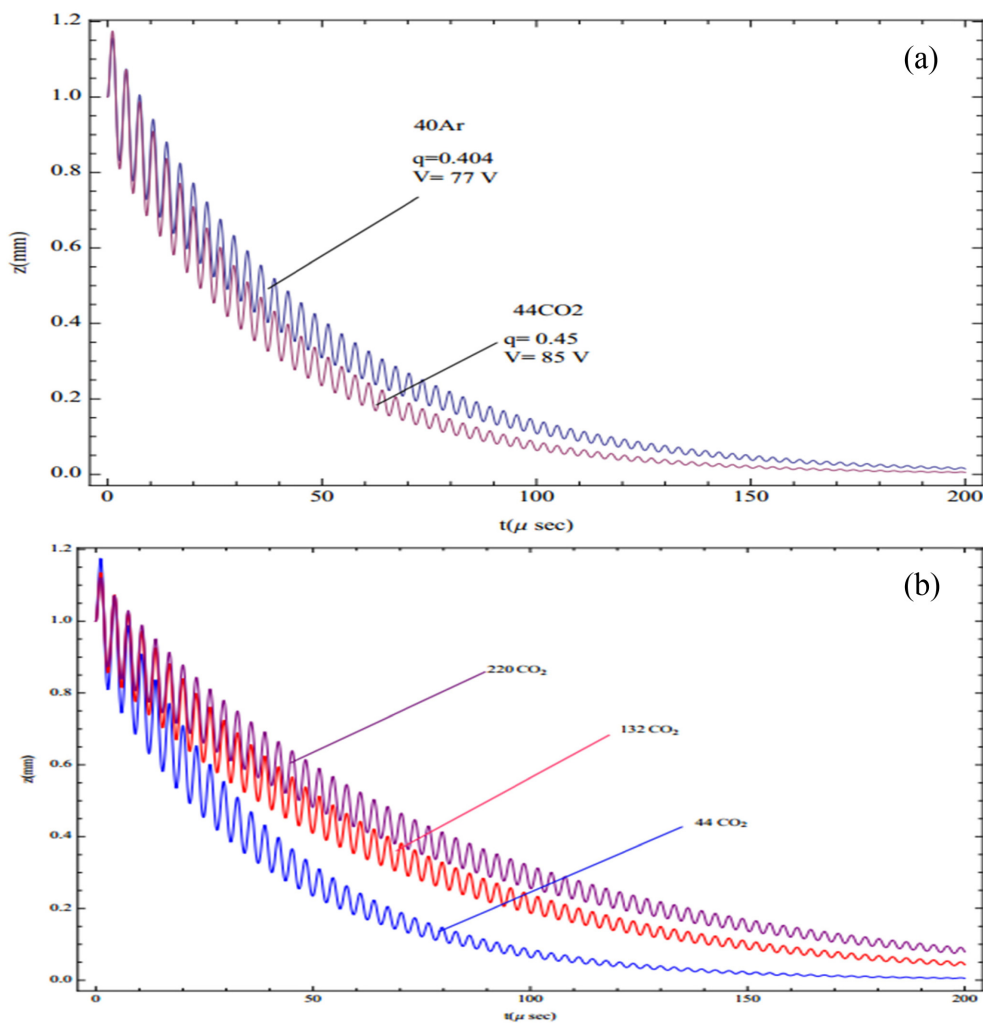


Figure 4. The confined of $^{40}\text{Ar}^+$ and $^{44}\text{CO}_2$ ions damping displacement as a function of damping time; the initial displacement: $q_z = 0.45$; $z(\xi_0) = 1 \text{ mm}$; $C = 1$; and $a_z = 0.4$. The confined off CO_2^+ , $\text{CO}_2^+(\text{CO}_2)_2$, $\text{CO}_2^+(\text{CO}_2)_4$, ion clusters damping displacement as a function of damping time; the initial displacement $z(\xi_0) = 1 \text{ mm}$; $C = 1$; and $a_z = 0.4$.

region. Figure 4(a) shows the obtained numerical computations for the initial ion displacement with a damping time of 200 μs for Ar^+ of mass $m = 40$ amu and $(\text{CO}_2)^+$ of mass $m = 44$ amu. Furthermore, Figure 4(b) also shows a very strong shift in the damping time when n values rising and gradually moves towards the stability limits $(\text{CO}_2^+(\text{CO}_2)_n, n = 0, 2, 4)$. This can be attributed to the energetic ion and instability of large clusters.

Conclusion

In this work, the condition of $\text{CO}_2^+(\text{CO}_2)_n$ cluster ion formation in a Paul ion trap has been studied. First, we have ionized Ar buffer gas which transfer Ar^+ charge to CO_2 molecules. The process of joining CO_2^+ ions to another CO_2 molecules usually take place in few. Although $\text{CO}_2^+(\text{CO}_2)_n$ have a large rate constant, nevertheless, the values of n in $\text{CO}_2^+(\text{CO}_2)_n$ cluster ions depended on the pressure of both the buffer gas and the main gas.

As the collisional cooling of CO_2^+ take place, the mixture of Ar- CO_2 peaks are observed and finally, cluster formation occurs. Based on damping time of clusters, the formation of clusters up to $n = 11$ by increasing the number of carbon dioxide molecules is complicated, the isomers structure would be manifold and complex. In some experiments, when the rf voltage is stopped, we have observed heavier cluster ions. This can be attributed to the cloud beam formation.

References

1. March, R. E. *J. Mass Spectrom.* **1997**, 32, 351.
2. Sadat Kiai, S. M.; Elahi, M.; Adlparvar, S.; Nemati, N.; Shafaei, S. R.; Karimi, L. *Mass Spectrom. Lett.* **2015**, 6, 112.
3. Kalkan, Y.; Arslanok, M.; Cortez, A. F. V.; Kaya, Y.; Tapan, I.; Veenhof, R. *J. Instrum.* **2015**, 10, 07004.
4. Heinbuch, S.; Dong, F.; Rocca, J. J.; Bernstein, E. R. *J. Chem. Phys.* **2006**, 125, 154316.
5. Johnston, R. *Atomic and molecular clusters*, Taylor and Francis: London, **2002**.
6. Wang, Y.-S.; Tsai, C.-H.; Lee, Y. T.; Chang, H.-C. *J. Phys. Chem. A* **2003**, 107, 4217.
7. Brédy, R.; Bernard, J.; Chen, L.; Montagne, G.; Li, B.; Martin, S. *J. Phys. B* **2009**, 42, 154023.
8. Pollack, S.; Cameron, D.; Rokni, M.; Hill, W.; Parks, J. H.; *Chem. Phys. Lett.* **1996**, 256, 101.
9. Jovan Jose, K. V.; Gadre, S. R. *J. Chem. Phys.* **2008**, 128, 124310.
10. Lovejoy, E.; Bianco, R.; *J. Phys. Chem. A* **2000**, 104, 10280.
11. Brédy, R.; Bernard, J.; Chen, L.; Montagne, G.; Li, B.; Martin, S. *J. Phys. B* **2009**, 42, 154023.
12. Brown, L. S.; Gabrielse, G. *Rev. Mod. Phys.* **1986**, 58, 233.
13. Paul, W. *Rev. Mod. Phys.* **1990**, 62, 531.
14. Bernhardt, T. M. *Int. J. Mass Spectrom.* **2005**, 243, 1.
15. Adersen, J. U.; Anersen, L. H.; Hvelplund, P.; Lapiere, A.; Moller, S. P.; Nielsen, S. B.; Pedersen, U. V.; Tomita S. *Hyperfine Interact.* **2003**, 146, 283.
16. Diner, A.; Toker, Y.; Strasser, D.; Heber, O.; Ben-Itzhak, I.; Witte, P. D.; Wolf, A.; Schwalm, D.; Rappaport, M. L.; Bhushan, K. G.; Zajfman, D. *Phys. Rev. Lett.*, **2004**, 93, 063402.
17. Schmidt, H. T.; Cederquist, H.; Jensen, J.; Fardi, A. *Nucl. Instrum. Methods Phys. Res. B* **2001**, 173, 523.
18. Overlay, O.; Ikezoe, Y.; Overlay, O.; Shimizu, S.; Sato, S.; Matsuoka, S.; Nakamura H.; Tamura, T. *Radiat. Phys. Chem.* **1982**, 20, 253.
19. Gerlich, D. *The Production and Study of Ultra-Cold Molecular Ions*, Chapter 6, world scientific publishing Ltd: London. **2008**.
20. Kiyania, A.; Abdollahzadeha, M.; Sadat Kiaib, S. M.; Zirak, A. R. *J. fusion energy* **2011**, 30, 291.
21. Colby, S. M.; Reilly, J. P. *Time-of-Flight Mass Spectrometry and its Applications*, Elsevier: Amsterdam, **1994**, 125.
22. Anicich, V. G. *J. Phys. Chem.* **1993**, 22, 1469.
23. Rashit, A. B.; Werneck, P. *Z. Naturforsch.* **1979**, 34a, 1410.
24. Castleman, A. W.; Khanna, J.; Khanna, S. N. *J. Phys. Chem. C* **2009**, 113, 2664.